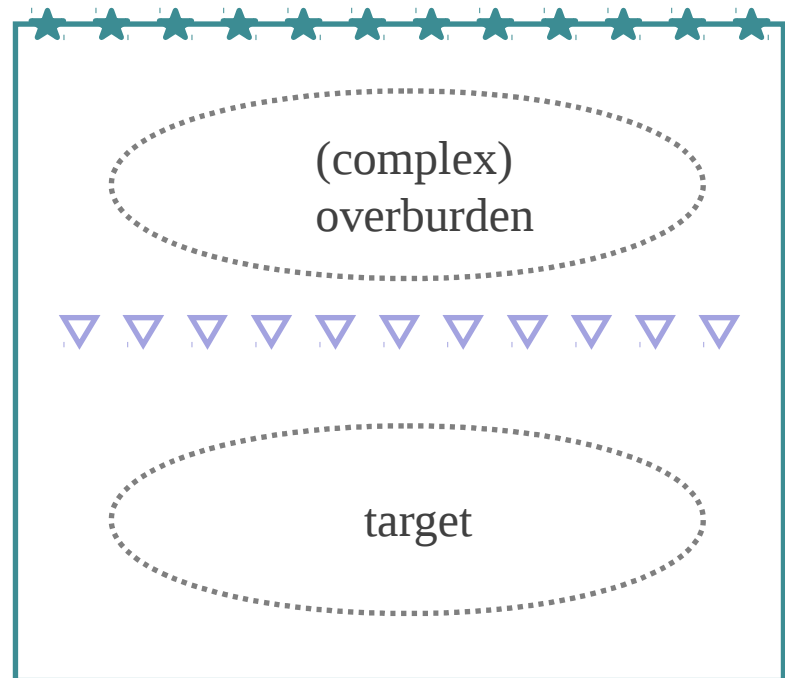
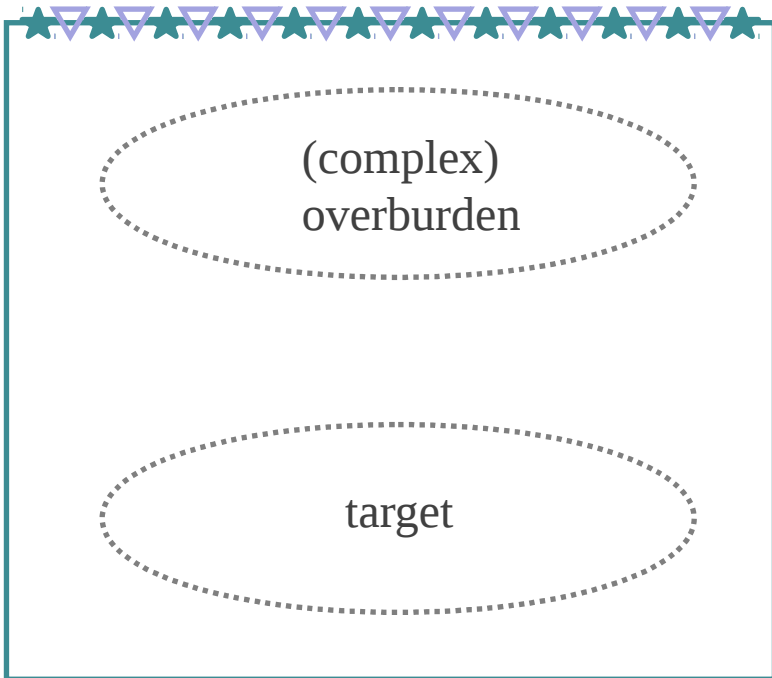


Combination of surface and borehole seismic data for robust target-oriented imaging

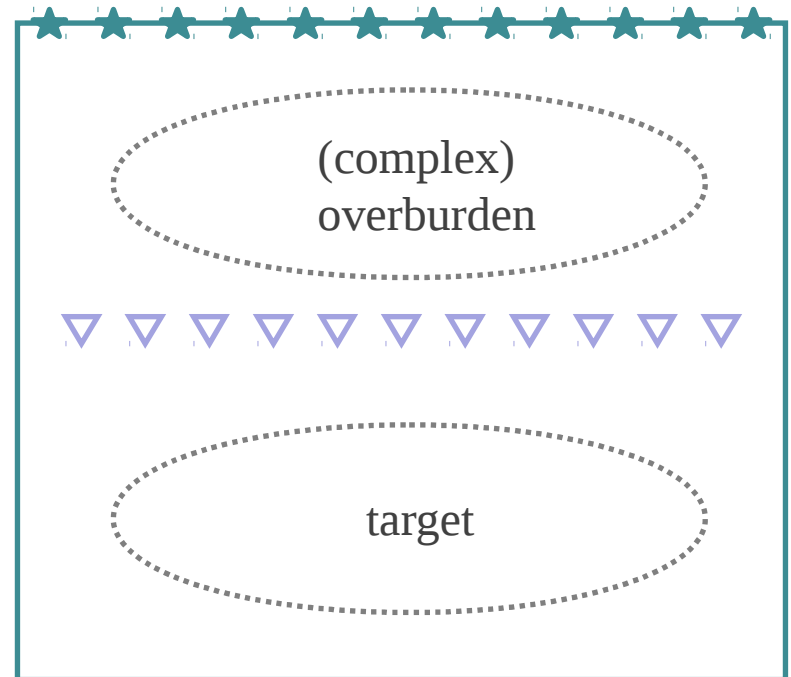
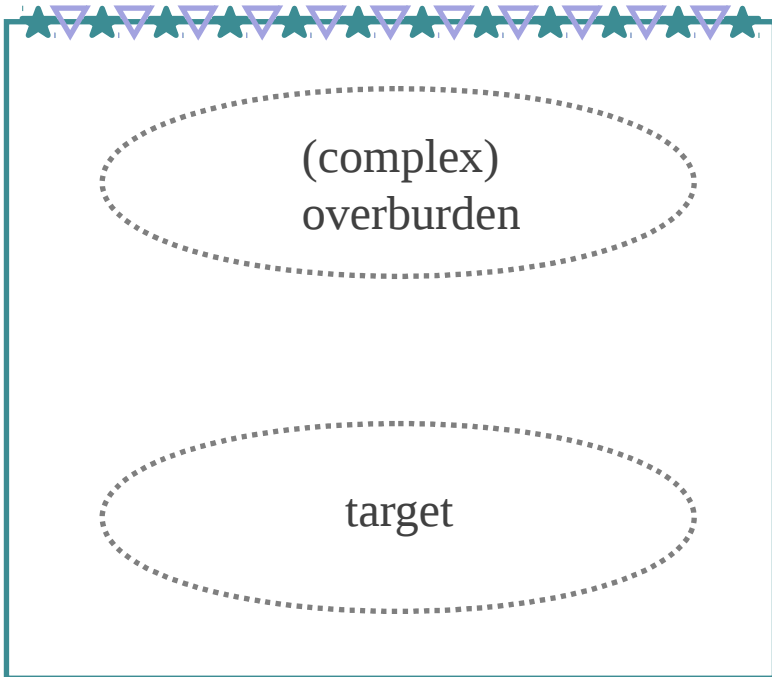
Yi Liu*, Norwegian University of Science and Technology
Joost van der Neut, Delft University of Technology
Børge Arntsen, Norwegian University of Science and Technology
Kees Wapenaar, Delft University of Technology

- Motivation
- Method
- Examples
- Conclusions

Motivation

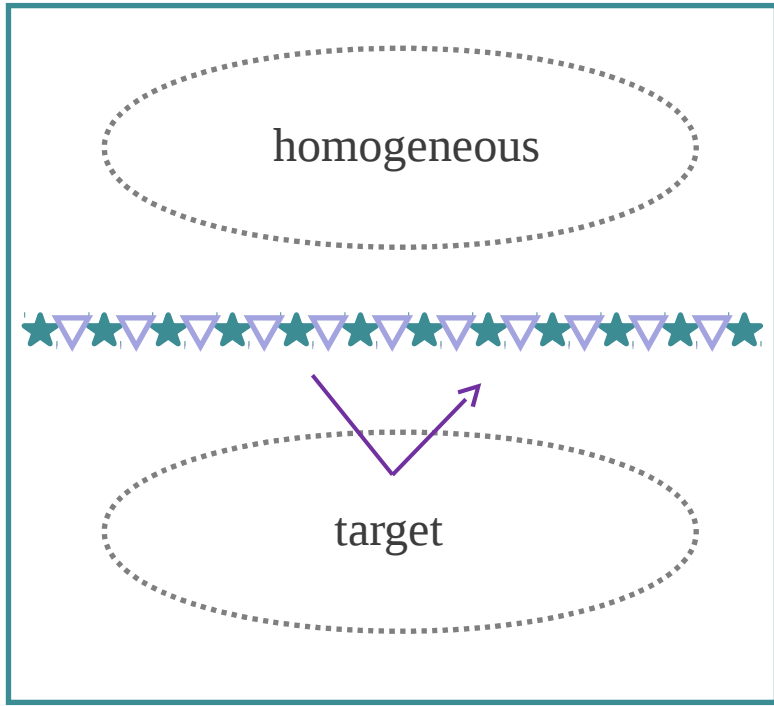


Motivation

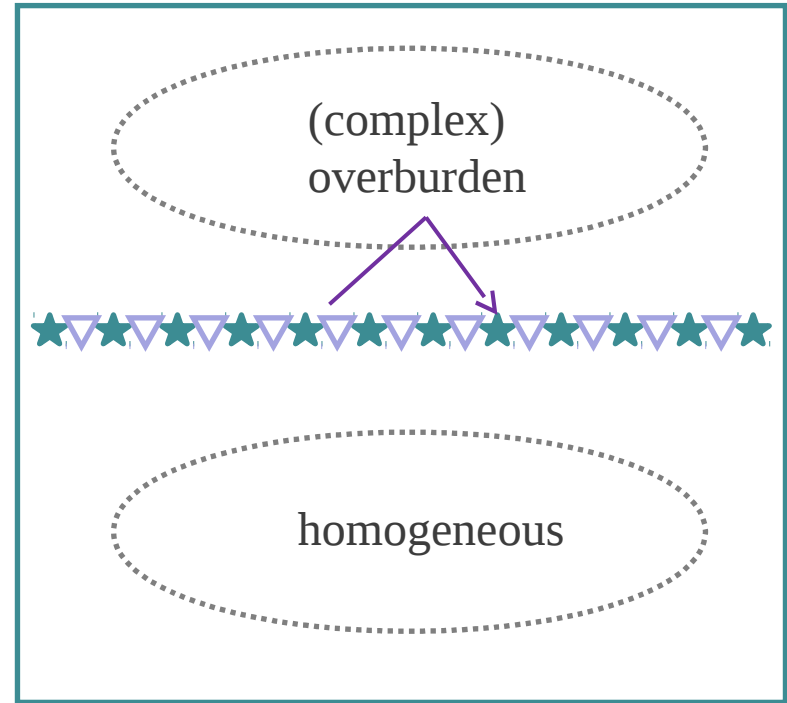
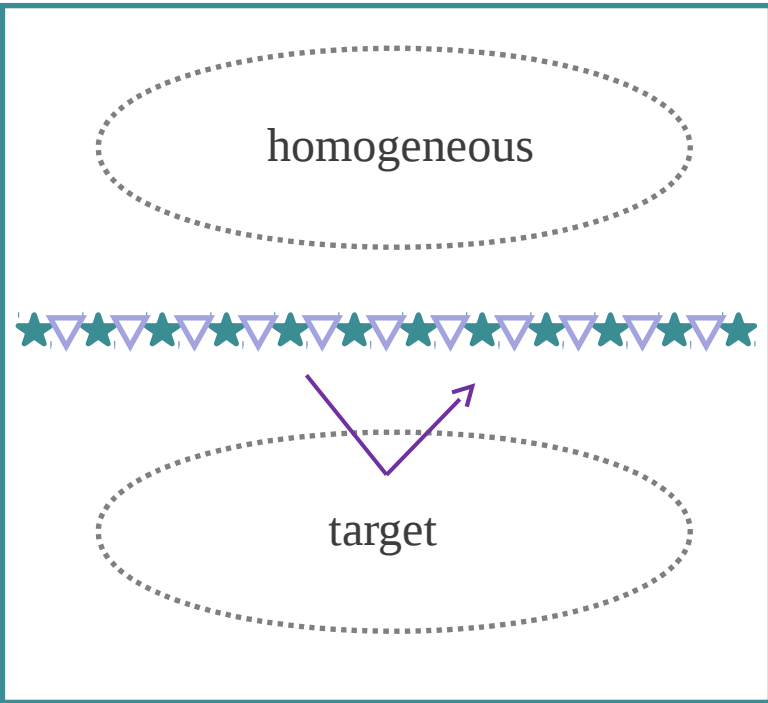


- A good velocity model of the **whole** area is crucial for imaging.

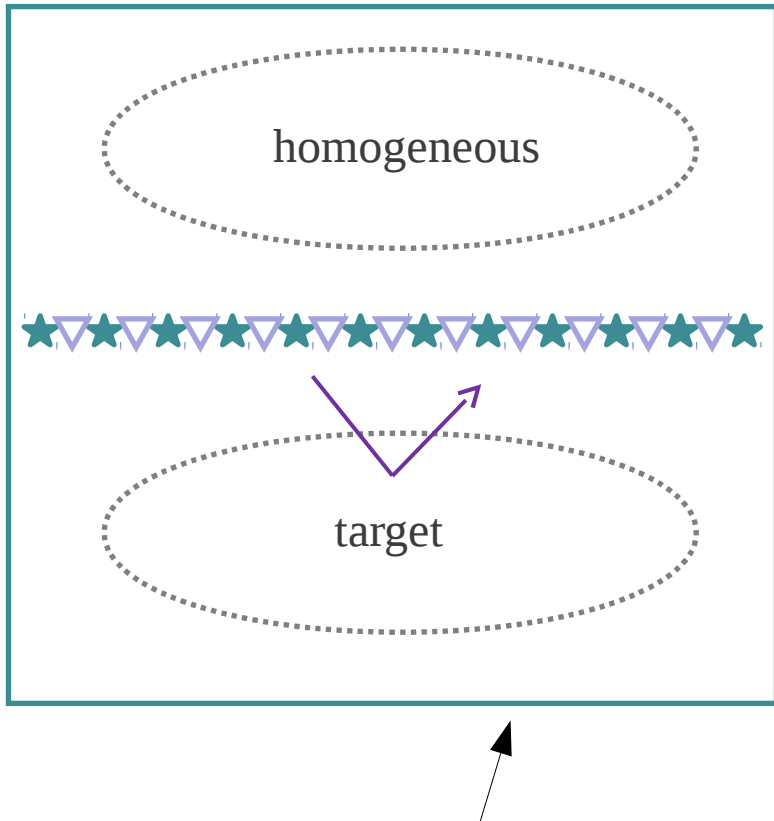
What if ...



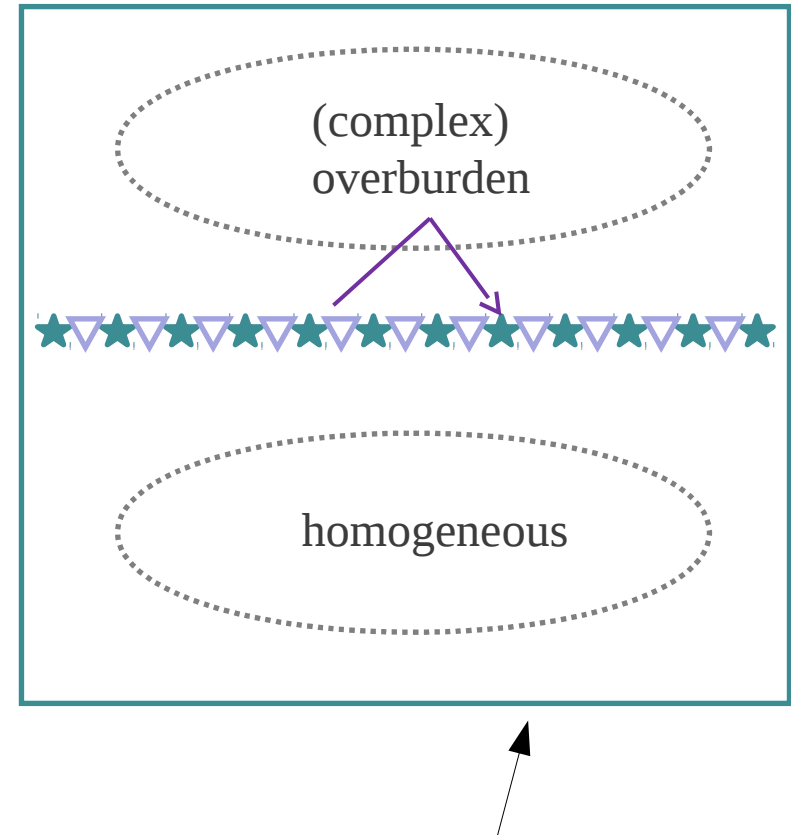
What if ...



What if ...



Imaging from **above**

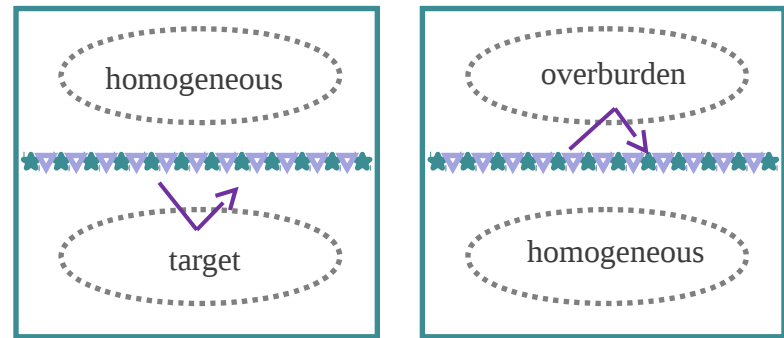


Imaging from **below**

Method

First **redatum**,

--> 2 new datasets



Method

First **redatum**,

--> 2 new datasets

then **image**...

--> only local velocities needed



Method

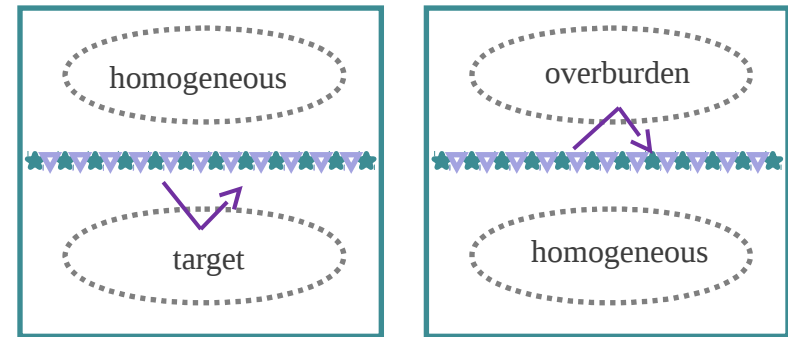
First **redatum**,

--> 2 new datasets

then **image**...

--> only local velocities needed

--> more robust to velocity errors



The two **new** datasets:

“R” from *above*

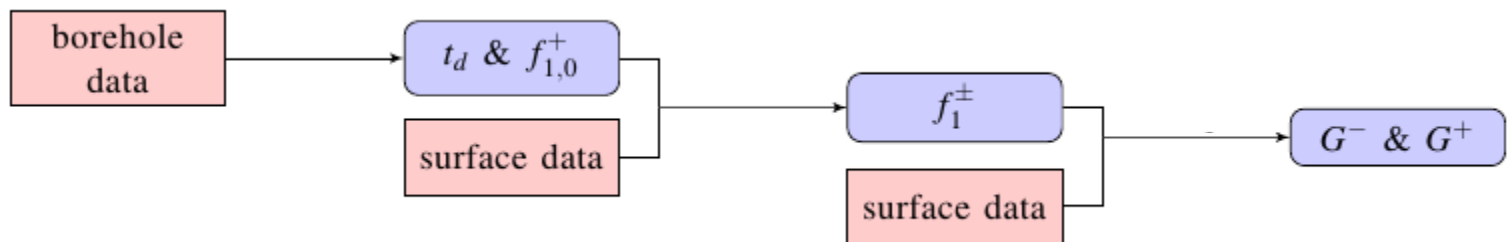
$$\widehat{G}^-(\mathbf{x}'_i | \mathbf{x}''_0) = \int_{\partial D_i} \widehat{\mathcal{R}}^\cup(\mathbf{x}'_i | \mathbf{x}_i) \widehat{G}^+(\mathbf{x}_i | \mathbf{x}''_0) d\mathbf{x}_i$$



The two new datasets:

“R” from *above*

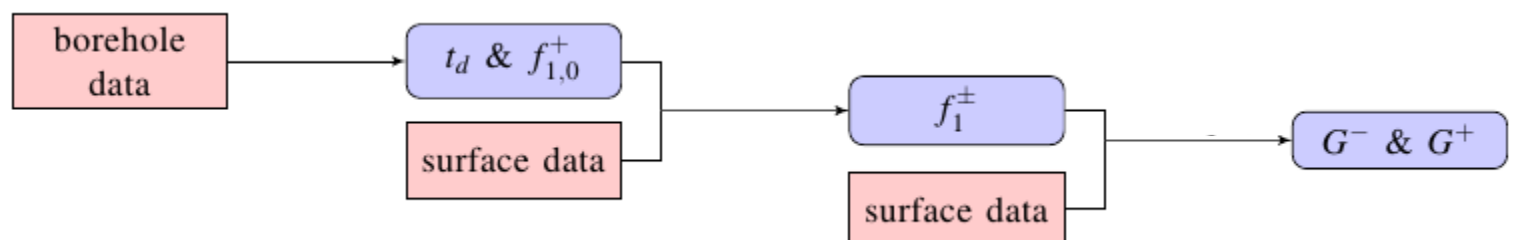
$$\widehat{G}^-(\mathbf{x}'_i | \mathbf{x}''_0) = \int_{\partial D_i} \widehat{\mathcal{R}}^\cup(\mathbf{x}'_i | \mathbf{x}_i) \widehat{G}^+(\mathbf{x}_i | \mathbf{x}''_0) d\mathbf{x}_i$$



The two new datasets:

“R” from *above*

$$\widehat{G}^-(\mathbf{x}'_i|\mathbf{x}''_0) = \int_{\partial D_i} \widehat{\mathcal{R}}^\cup(\mathbf{x}'_i|\mathbf{x}_i) \widehat{G}^+(\mathbf{x}_i|\mathbf{x}''_0) d\mathbf{x}_i$$



for $t < t_d(\mathbf{x}'_i|\mathbf{x}''_0)$,

$$f_1^-(\mathbf{x}''_0|\mathbf{x}'_i, t) = \int_{\partial D_0} \int_{-\infty}^t \mathcal{R}^\cup(\mathbf{x}''_0|\mathbf{x}_0, t - t') f_1^+(\mathbf{x}_0|\mathbf{x}'_i, t') dt' d\mathbf{x}_0;$$

for $t \geq t_d(\mathbf{x}'_i|\mathbf{x}''_0)$,

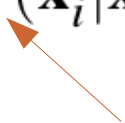
$$G^-(\mathbf{x}'_i|\mathbf{x}''_0, t) = \int_{\partial D_0} \int_{-\infty}^t \mathcal{R}^\cup(\mathbf{x}''_0|\mathbf{x}_0, t - t') f_1^+(\mathbf{x}_0|\mathbf{x}'_i, t') dt' d\mathbf{x}_0;$$

$$G^+(\mathbf{x}'_i|\mathbf{x}''_0, t) = - \int_{\partial D_0} \int_{-\infty}^t \mathcal{R}^\cup(\mathbf{x}''_0|\mathbf{x}_0, t - t') f_1^-(\mathbf{x}_0|\mathbf{x}'_i, -t') dt' d\mathbf{x}_0 + f_{1,0}^+(\mathbf{x}''_0|\mathbf{x}'_i, -t).$$

The two **new** datasets:

“R” from *below*

$$\widehat{f}_2^+(\mathbf{x}'_i|\mathbf{x}''_0) = \int_{\partial D_i} \widehat{\mathcal{R}}^\cap(\mathbf{x}'_i|\mathbf{x}_i) \widehat{f}_2^-(\mathbf{x}_i|\mathbf{x}''_0) d\mathbf{x}_i$$



The two **new** datasets:

To image from *below*

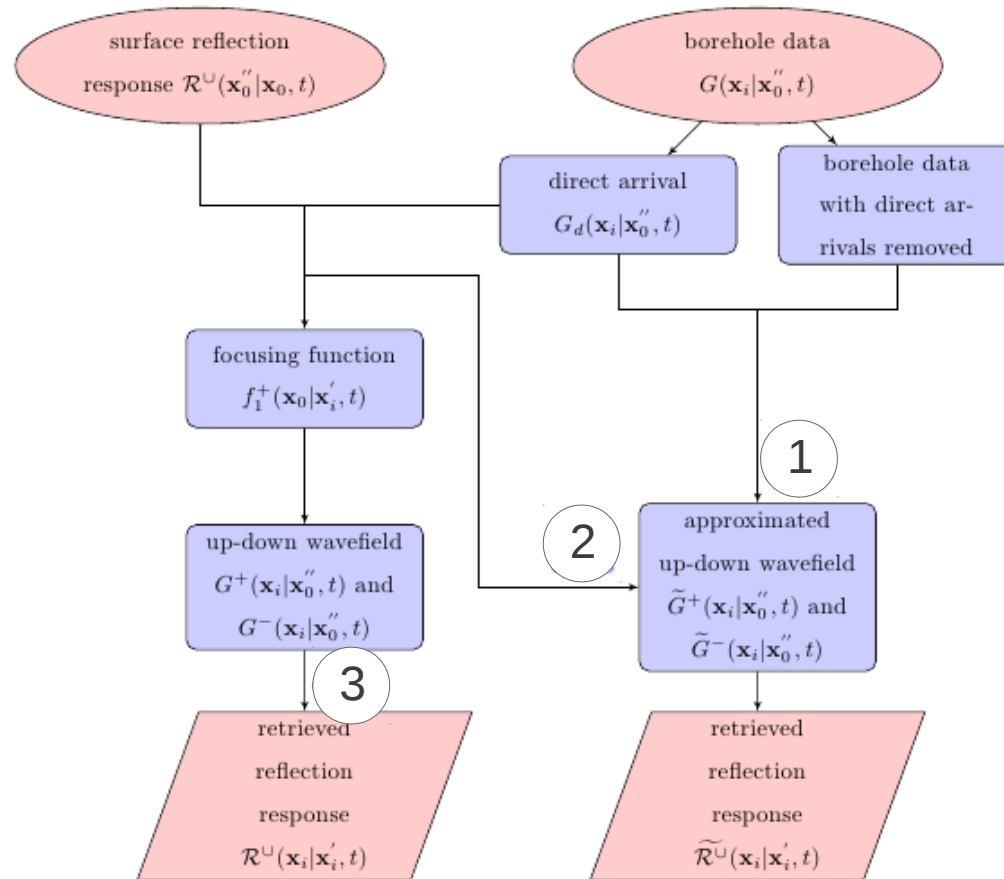
$$\widehat{f}_2^+(\mathbf{x}'_i|\mathbf{x}''_0) = \int_{\partial D_i} \widehat{\mathcal{R}}^\cap(\mathbf{x}'_i|\mathbf{x}_i) \widehat{f}_2^-(\mathbf{x}_i|\mathbf{x}''_0) d\mathbf{x}_i$$

$$f_1^+(\mathbf{x}''_0|\mathbf{x}'_i, t) = f_2^-(\mathbf{x}'_i|\mathbf{x}''_0, t);$$

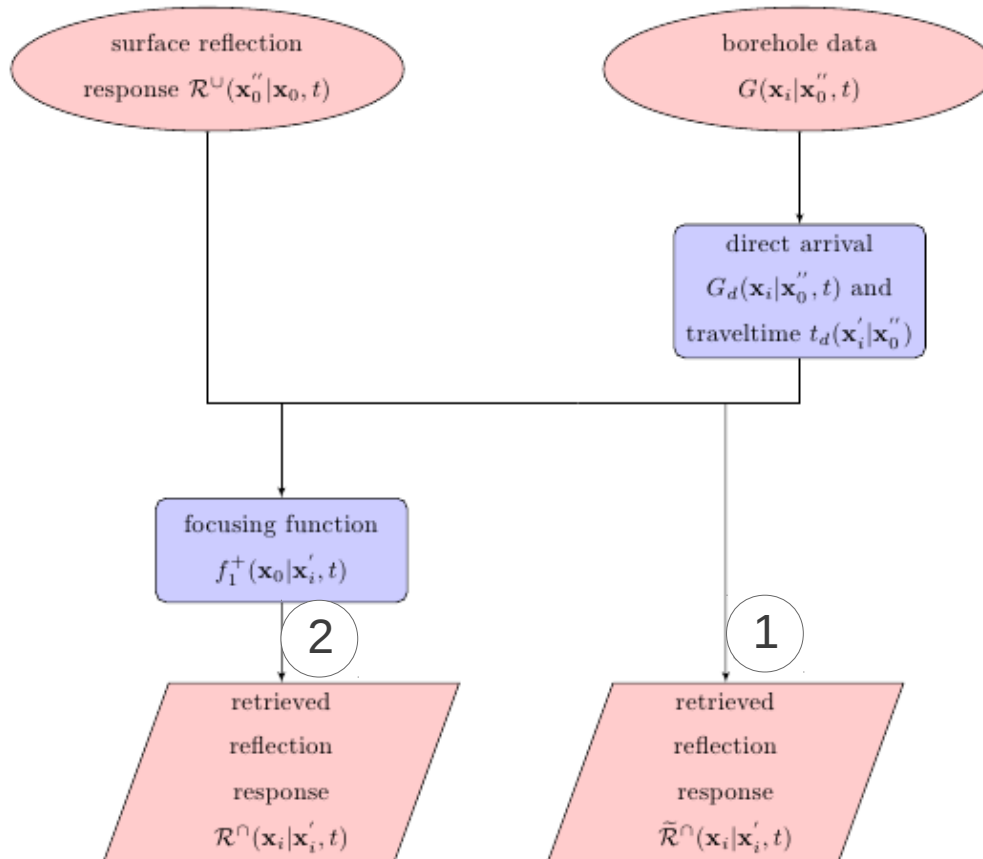
and

$$-f_1^-(\mathbf{x}''_0|\mathbf{x}'_i, -t) = f_2^+(\mathbf{x}'_i|\mathbf{x}''_0, t).$$

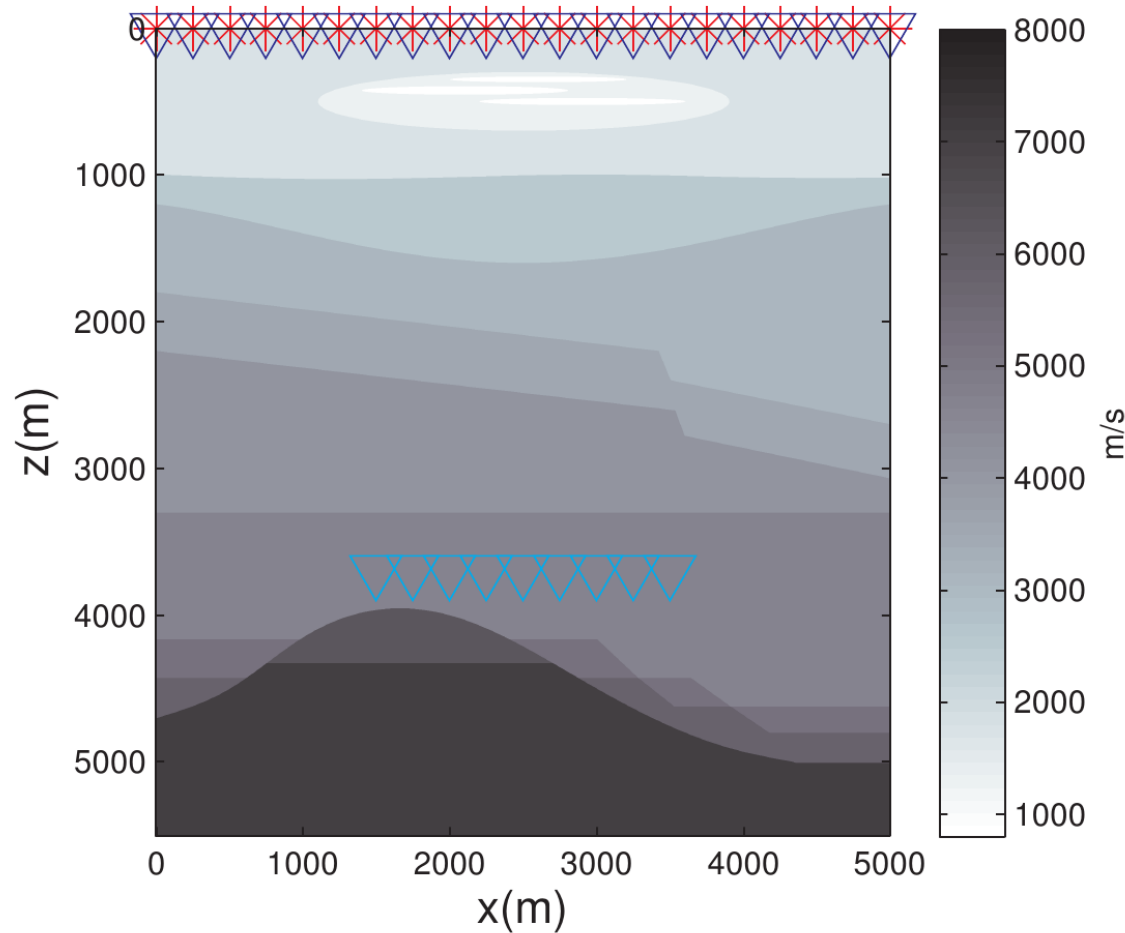
Flow chart for “R” from *above*



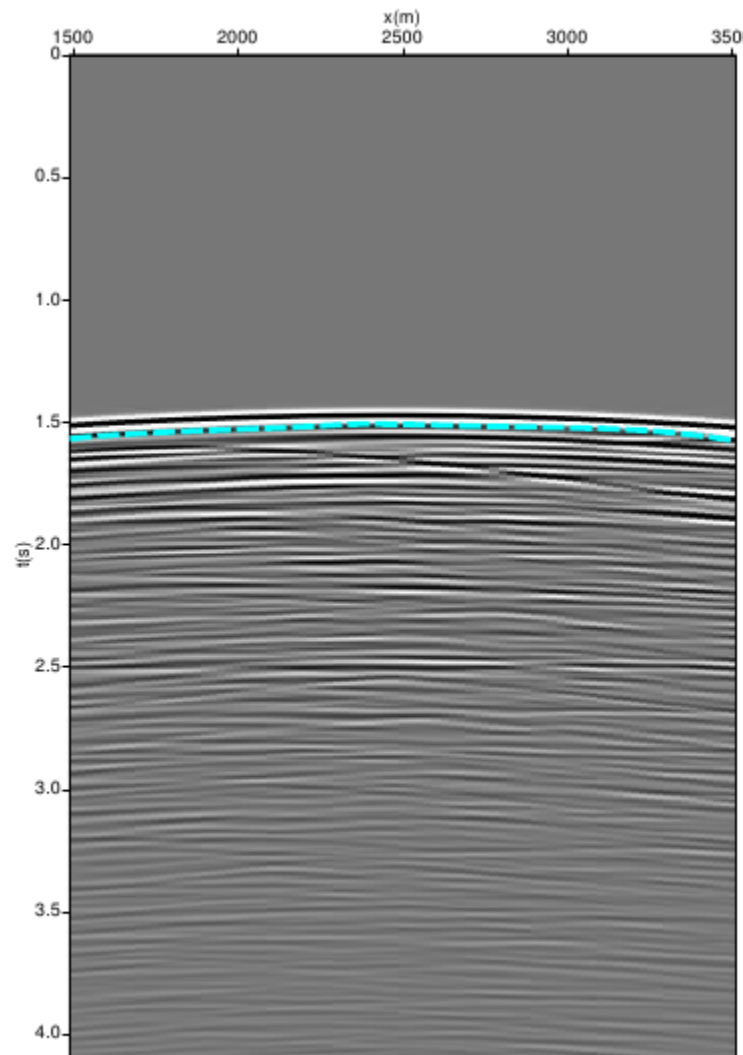
Flow chart for “R” from *below*



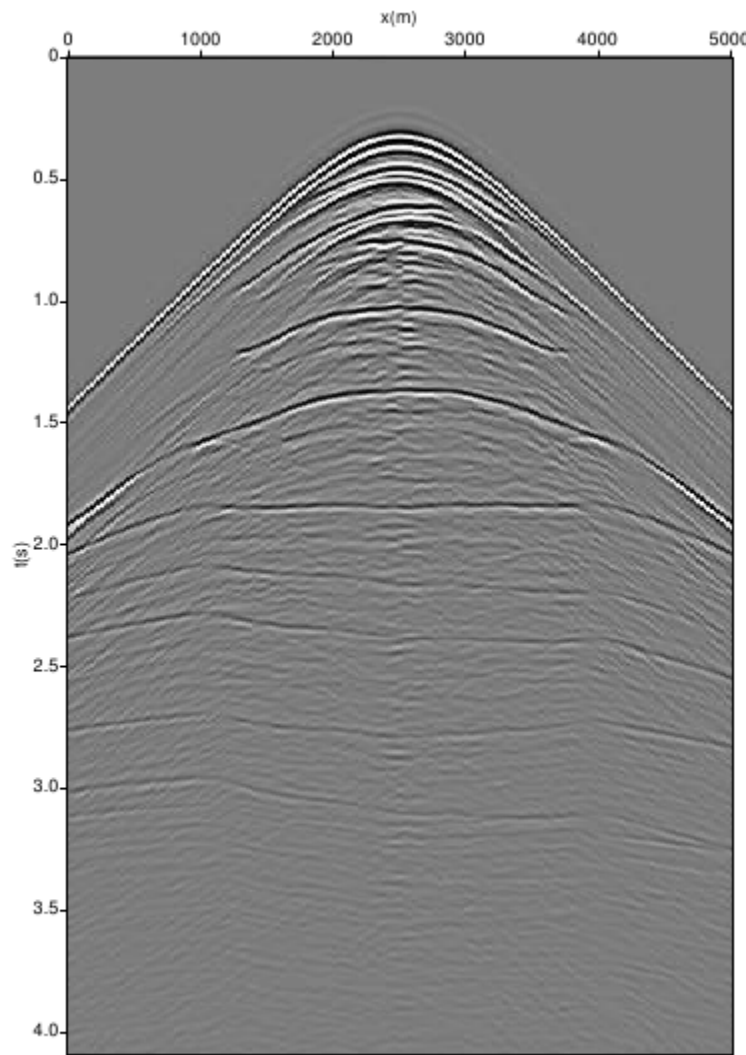
Example 1



Example 1

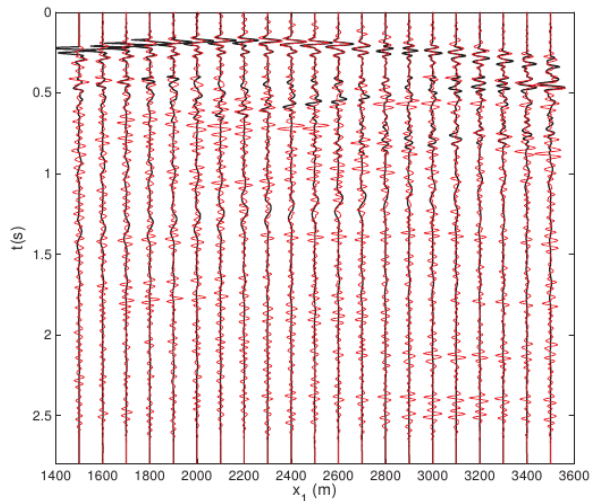


(a)

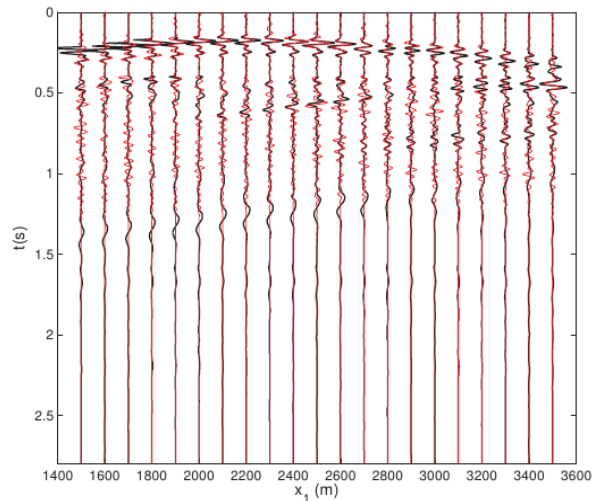


(b)

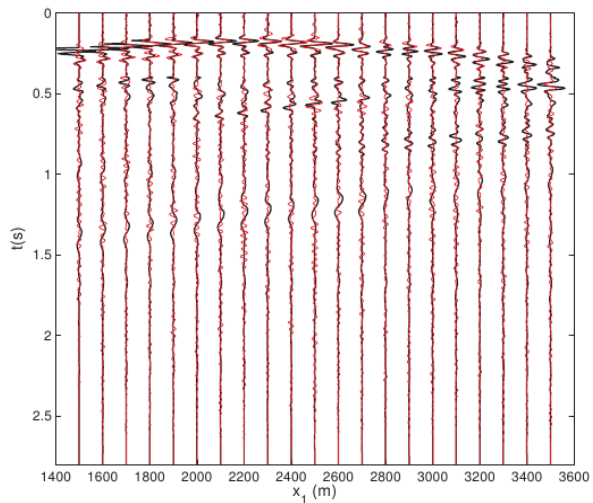
Example 1 – “R” (from *above*)



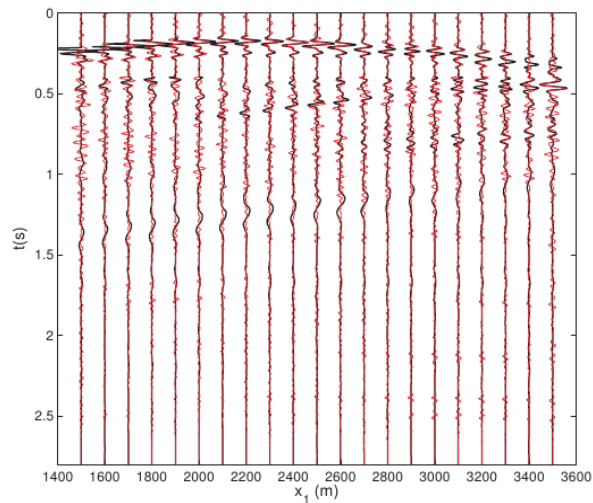
1



2

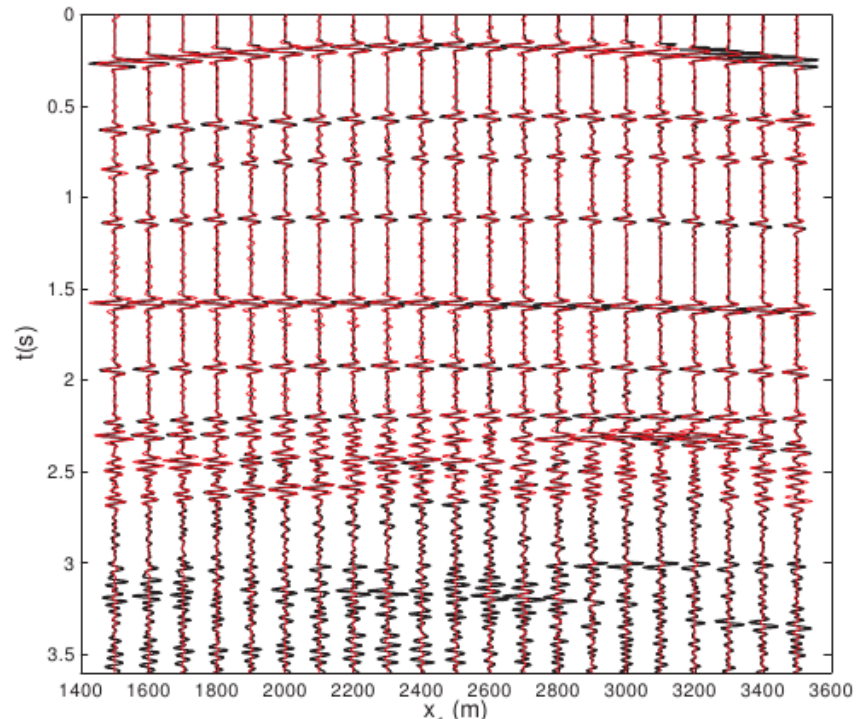
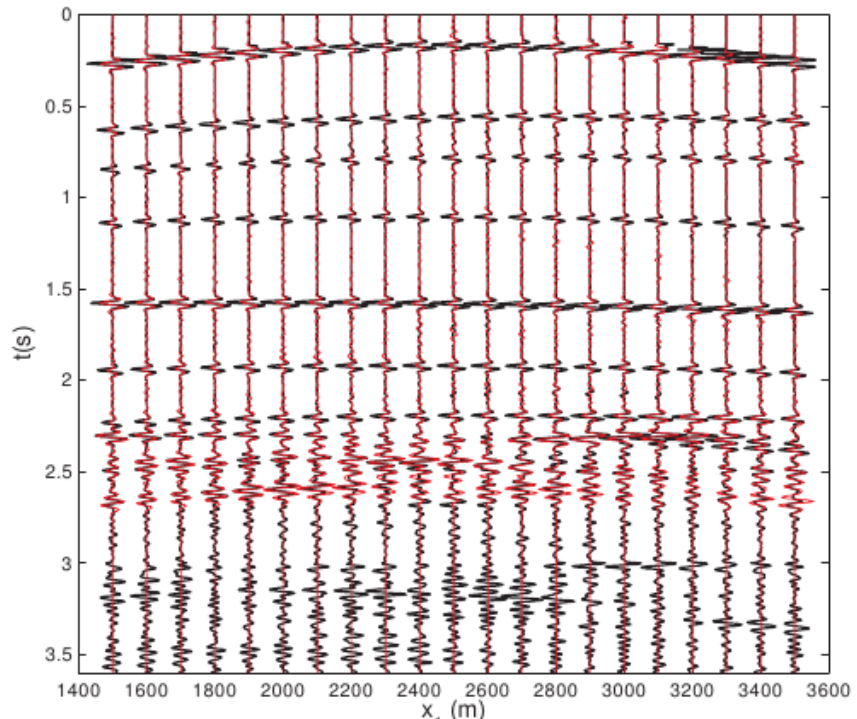


3

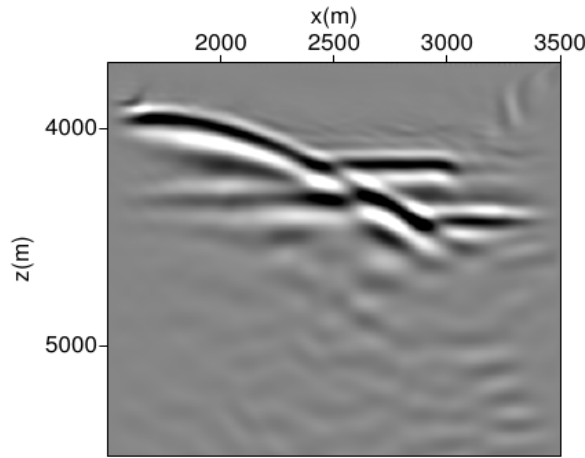


4

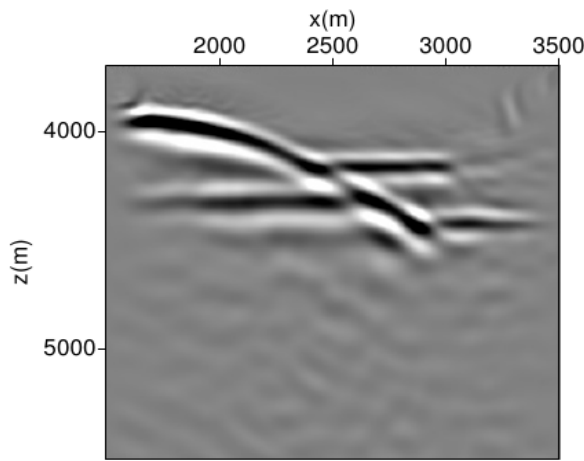
Example 1 – “R” (from *below*)



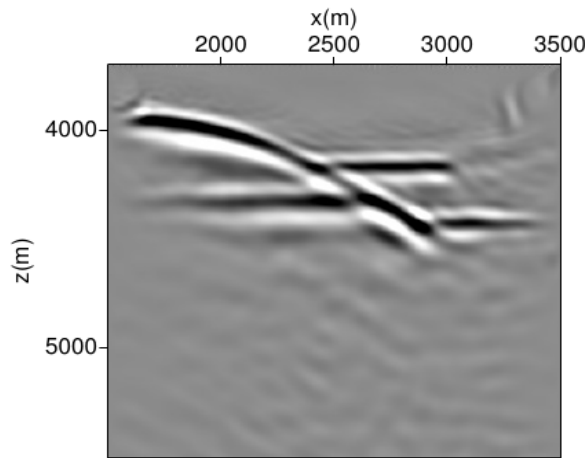
Example 1 – images (from *above*)



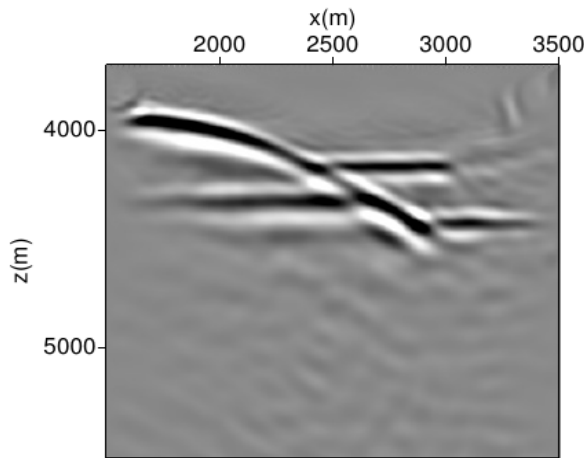
1



2

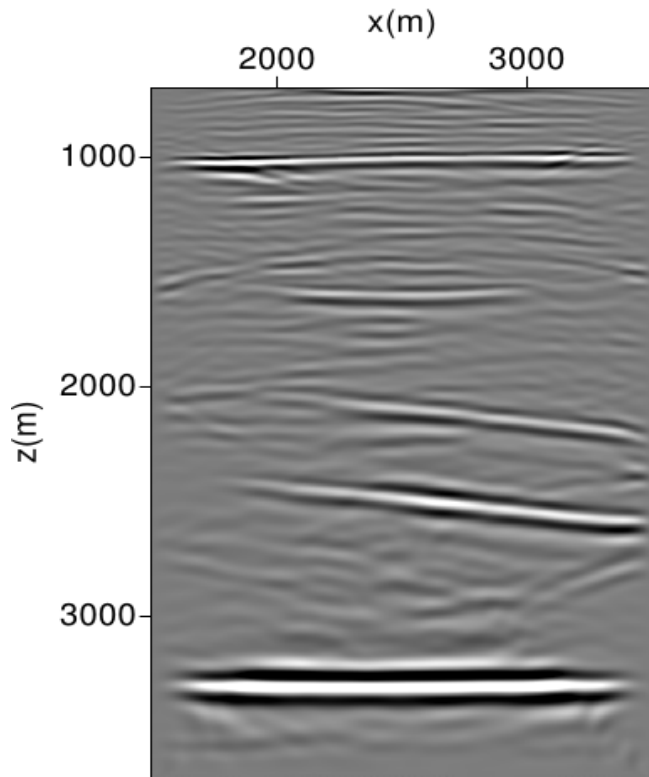


3

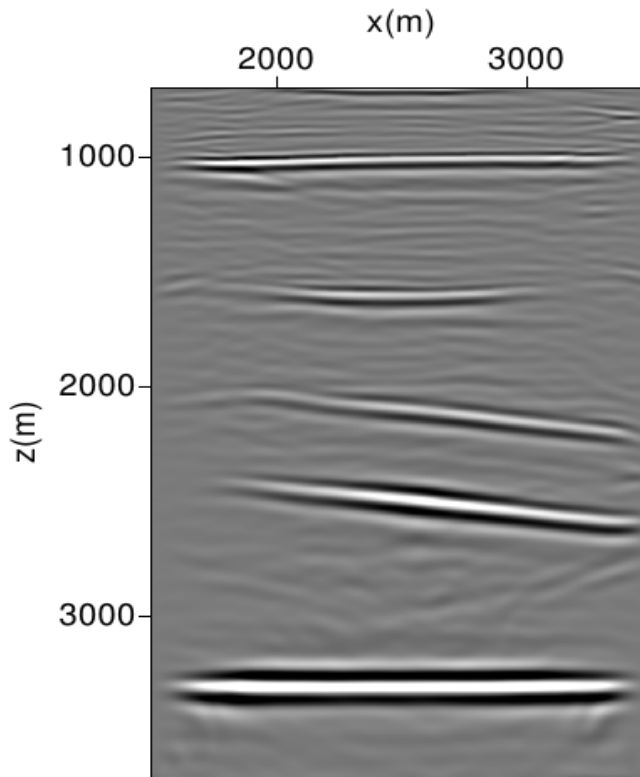


4

Example 1 – images (from *below*)

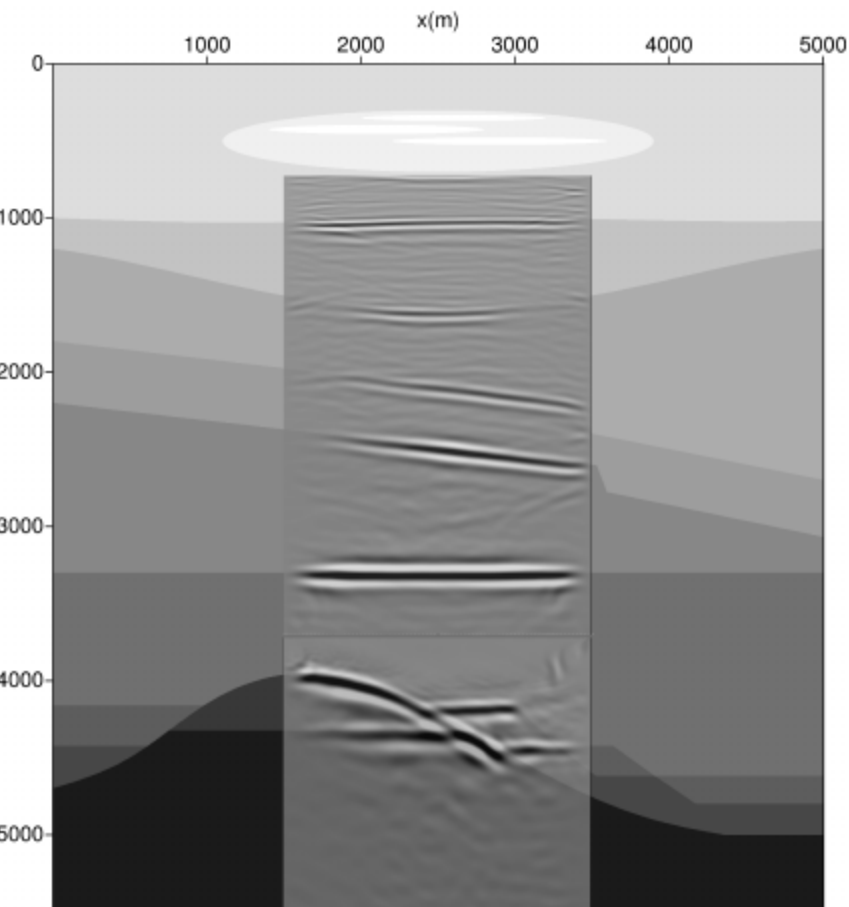


1



2

Example 1 – comparison (correct velocities)



Combined local image

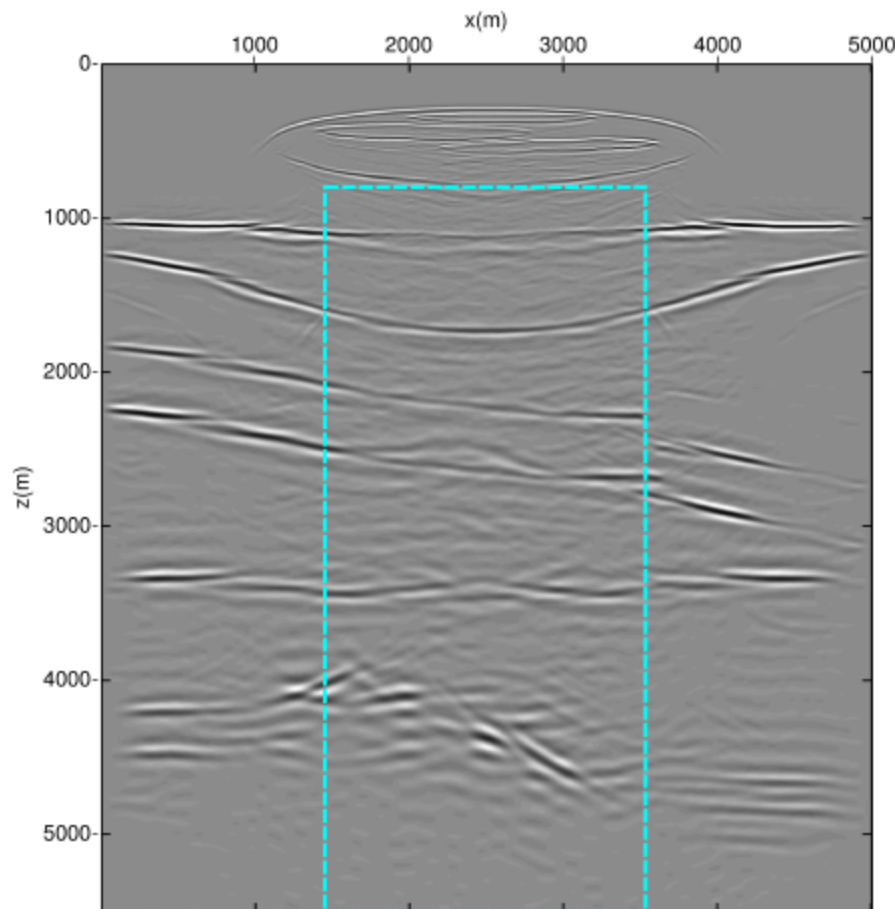
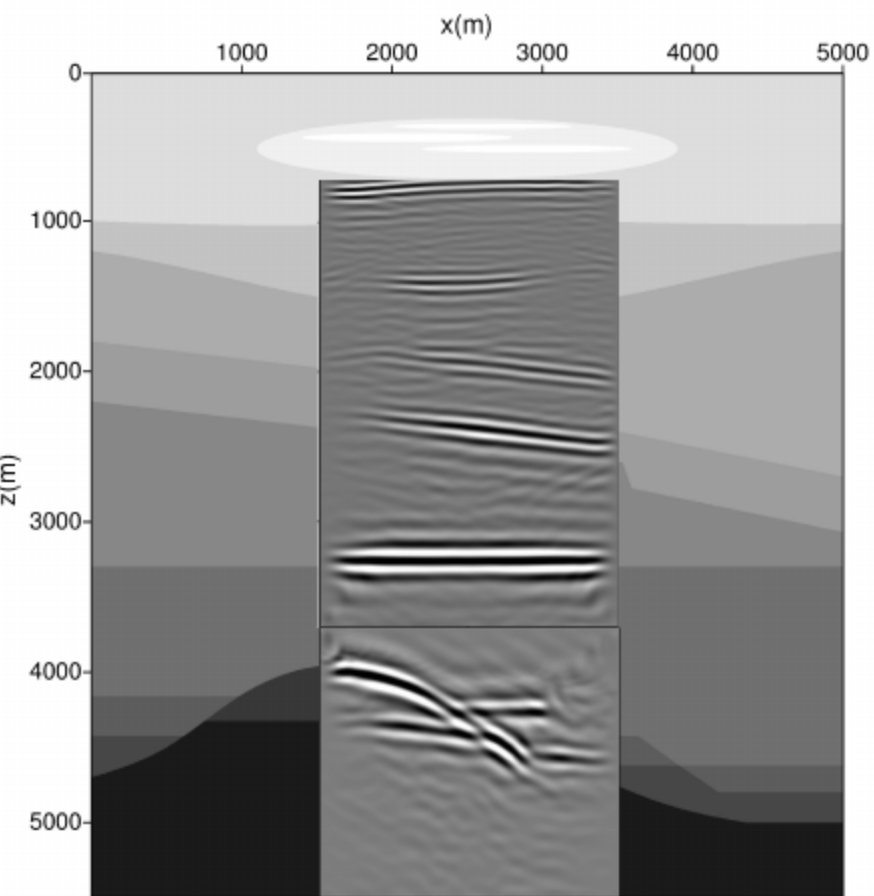


Image from the surface

Example 1 – comparison (wrong velocities)



Combined local image

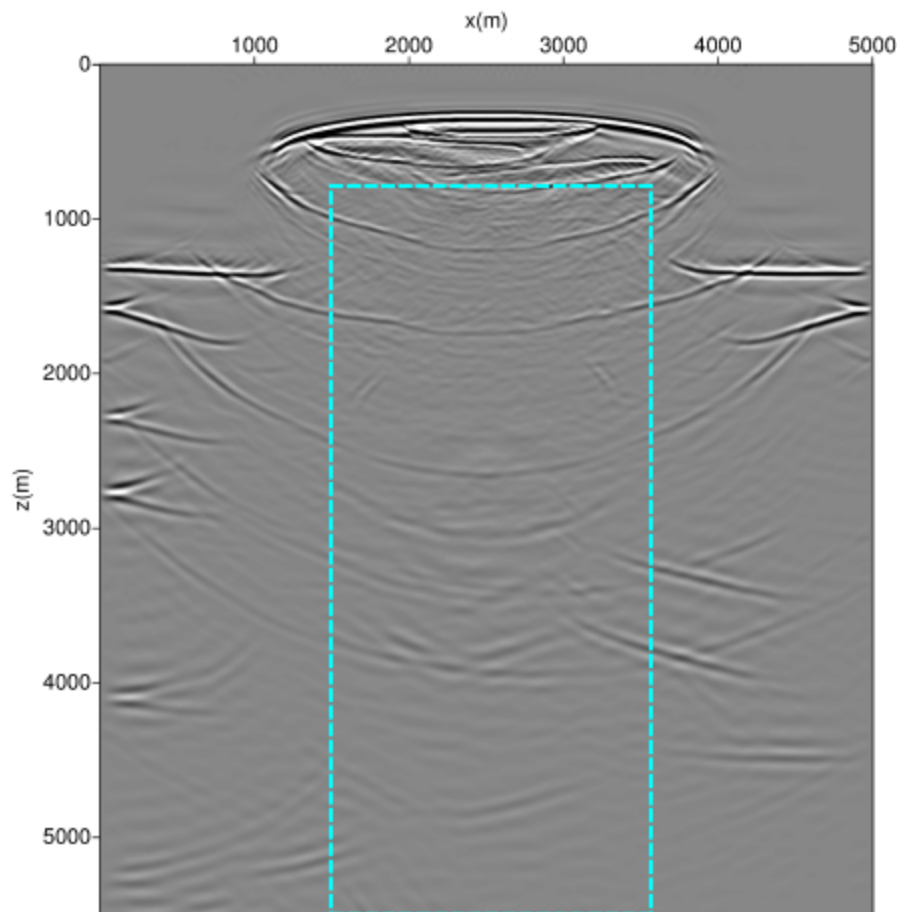
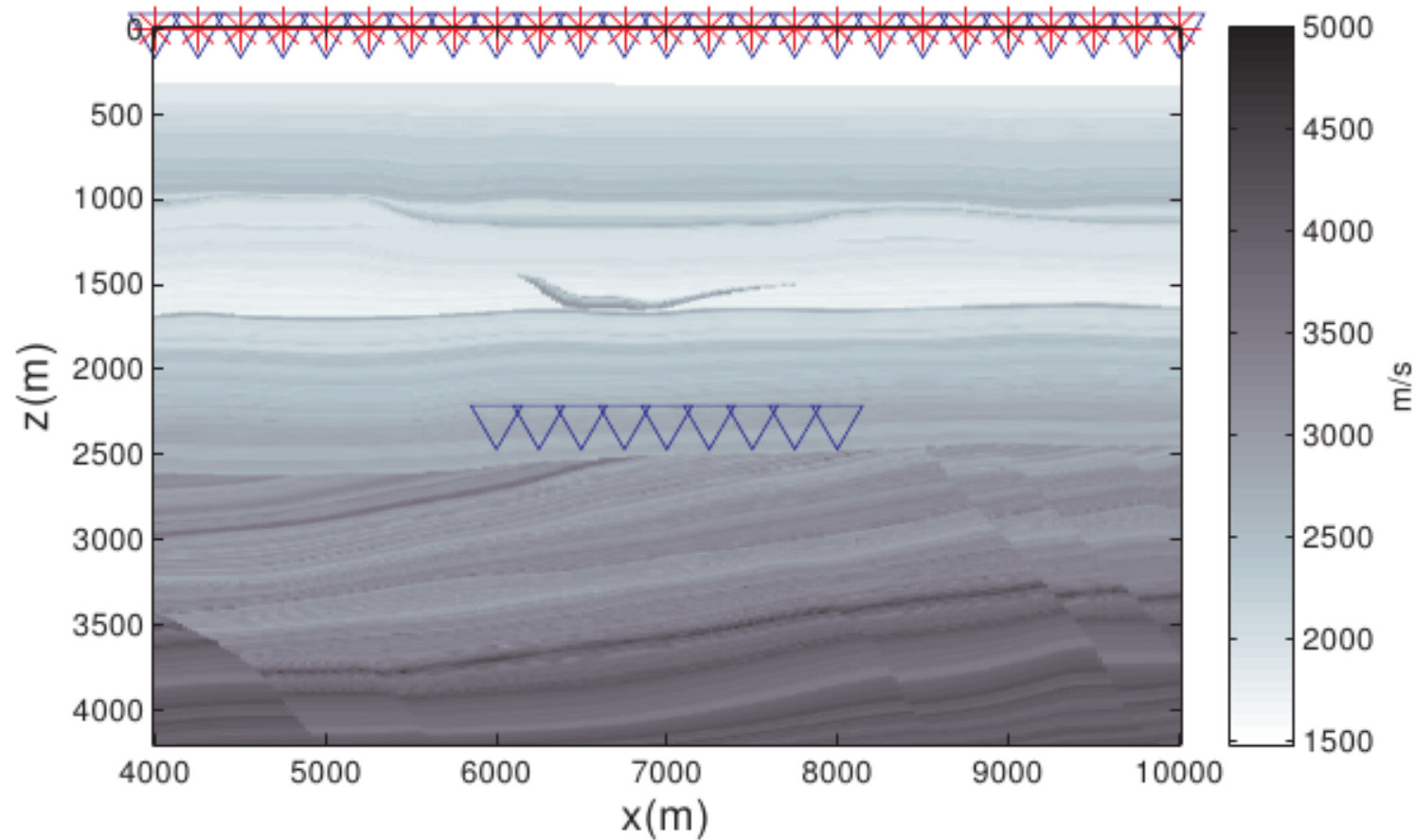
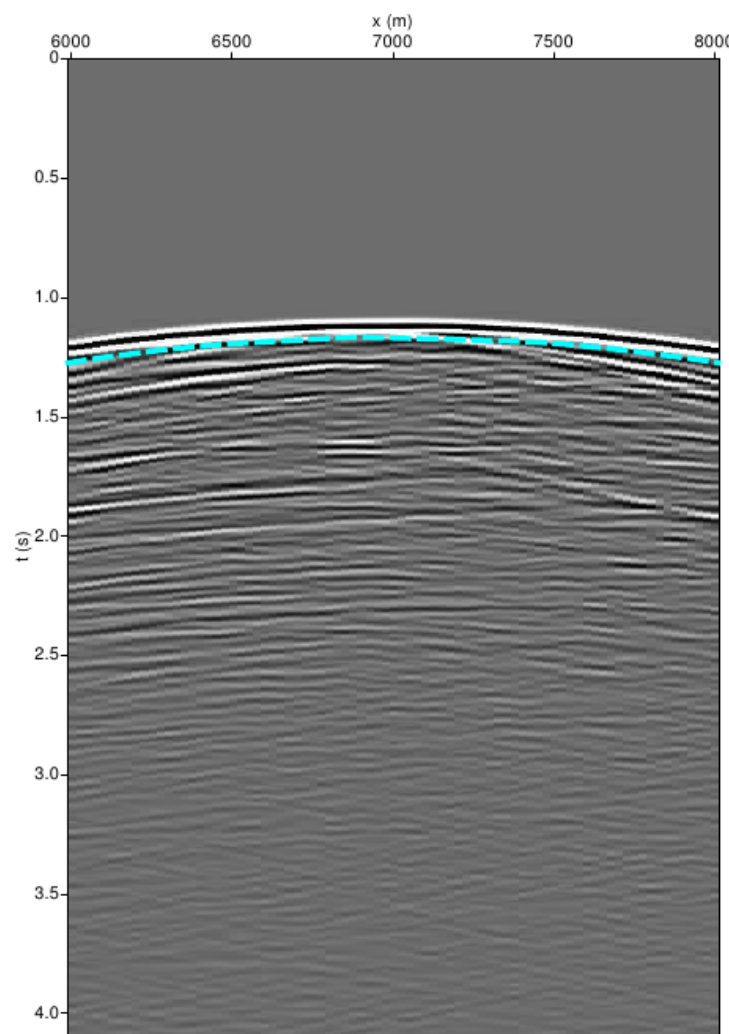


Image from the surface

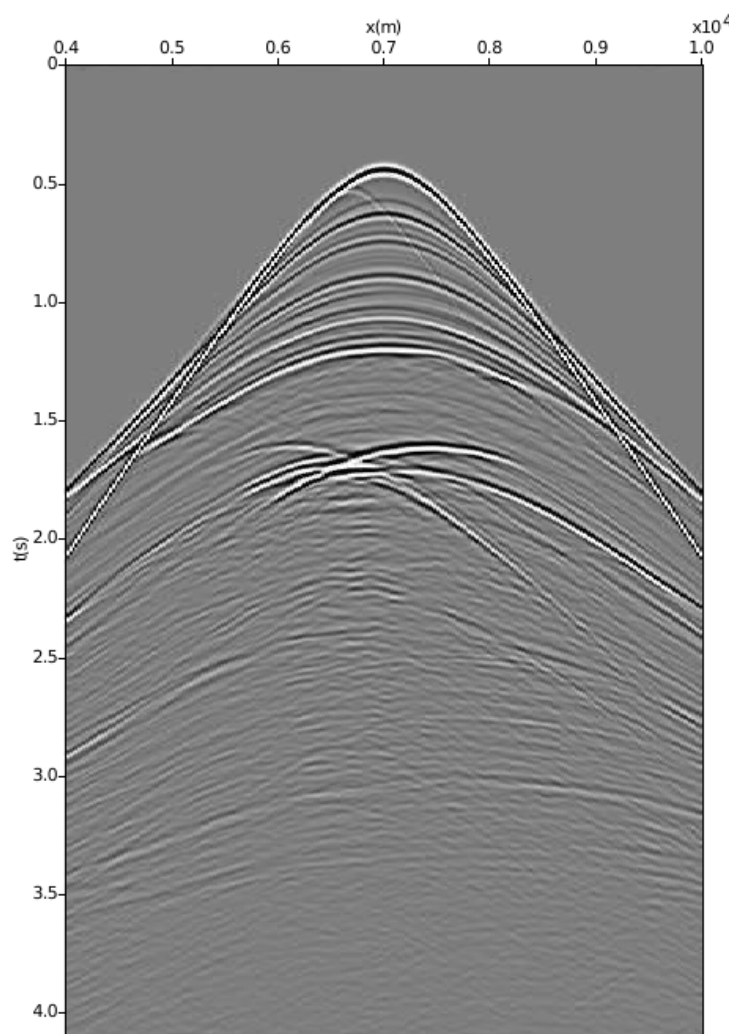
Example 2



Example 2

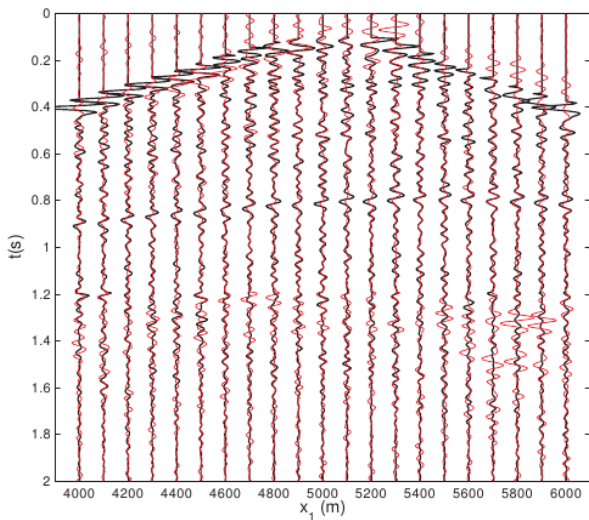


(a)

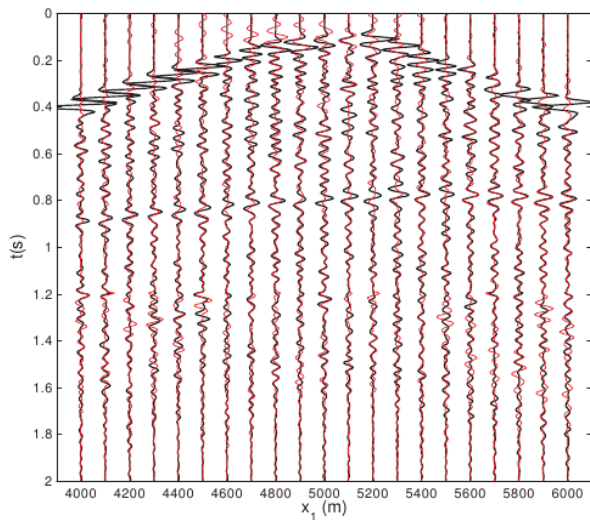


(b)

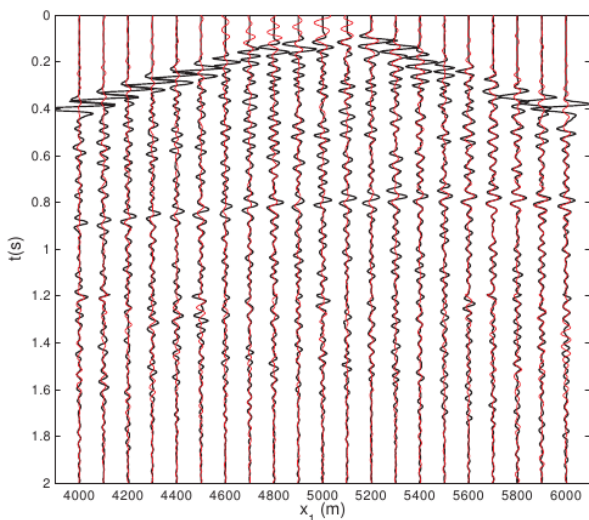
Example 2 – “R” from *above*



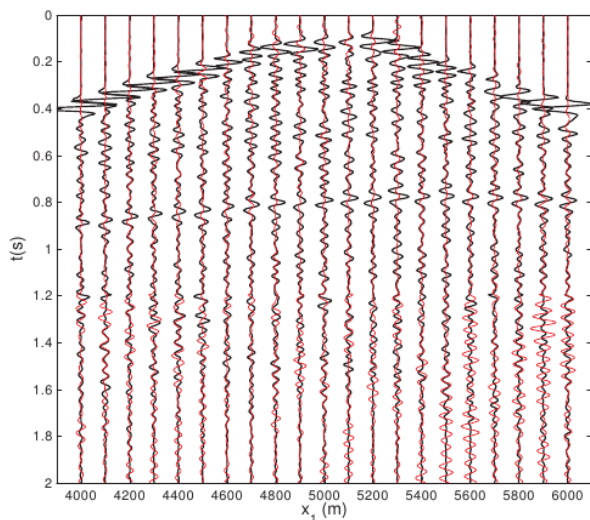
1



2

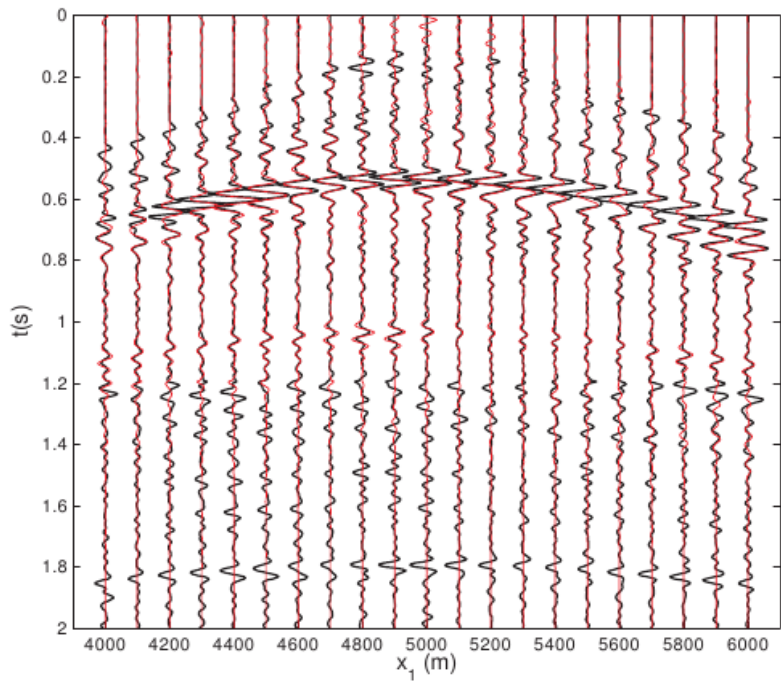


3

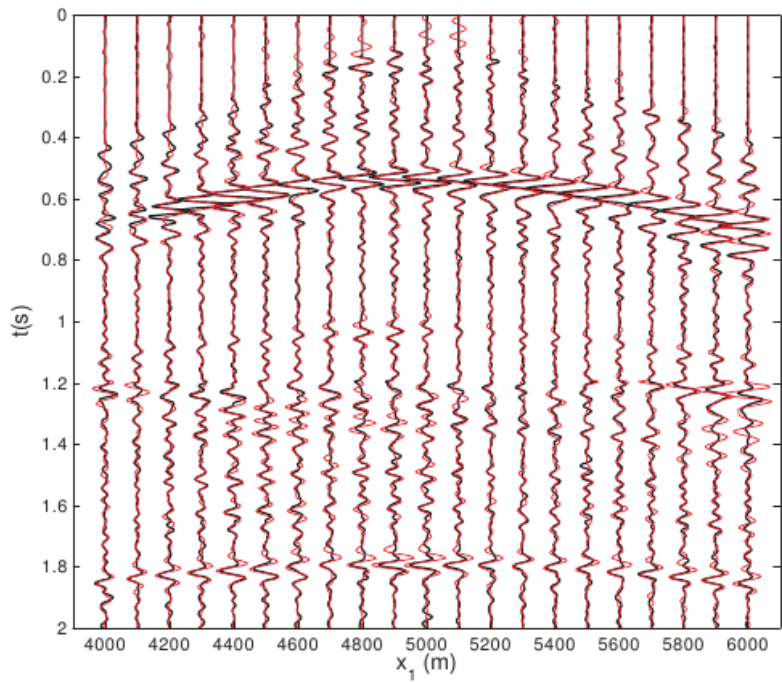


4

Example 2 – “R” from *below*

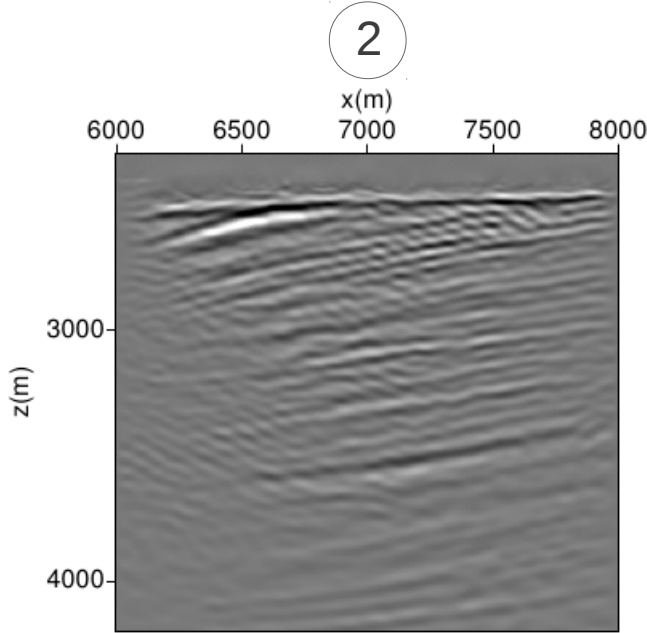
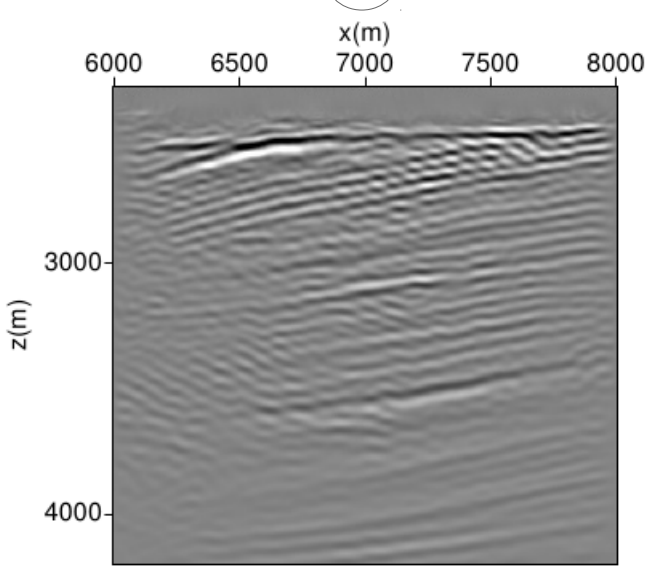
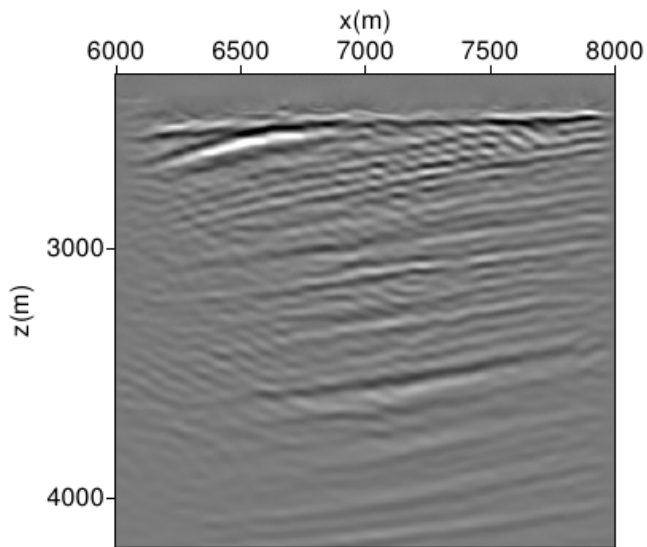
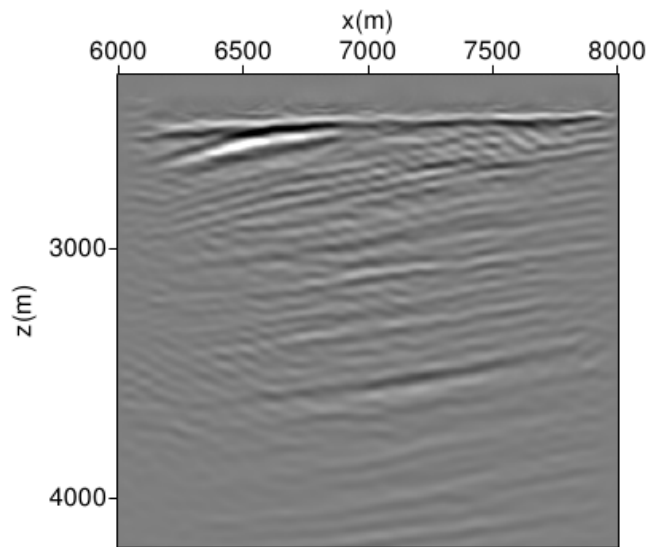


1

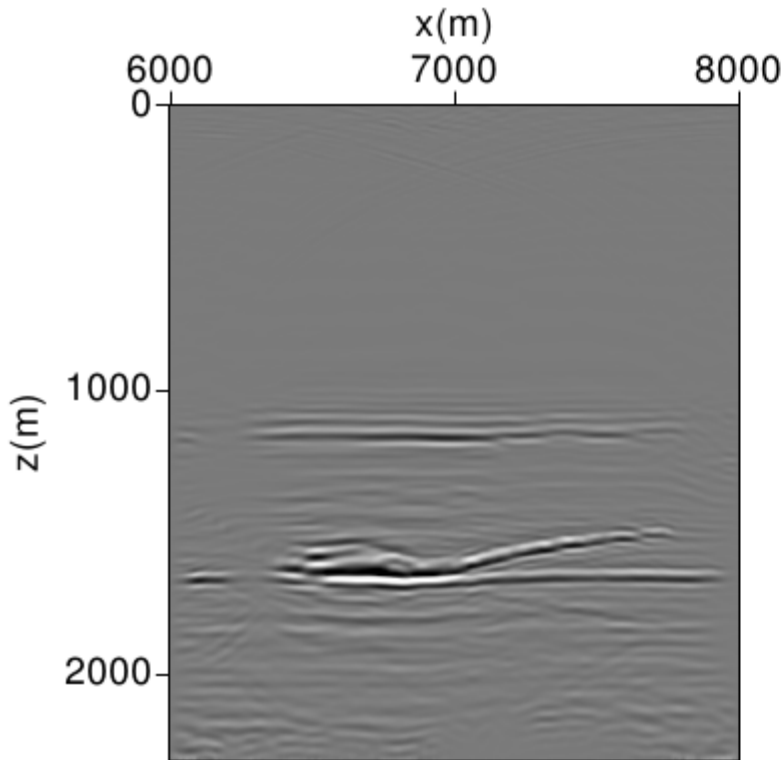


2

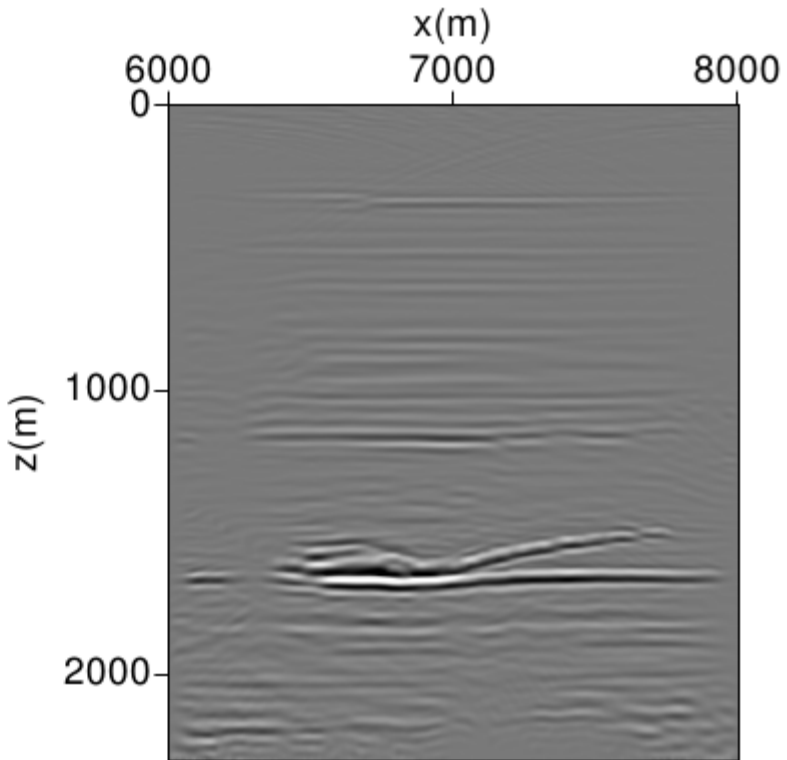
Example 2 – images from *above*



Example 2 – images from *below*

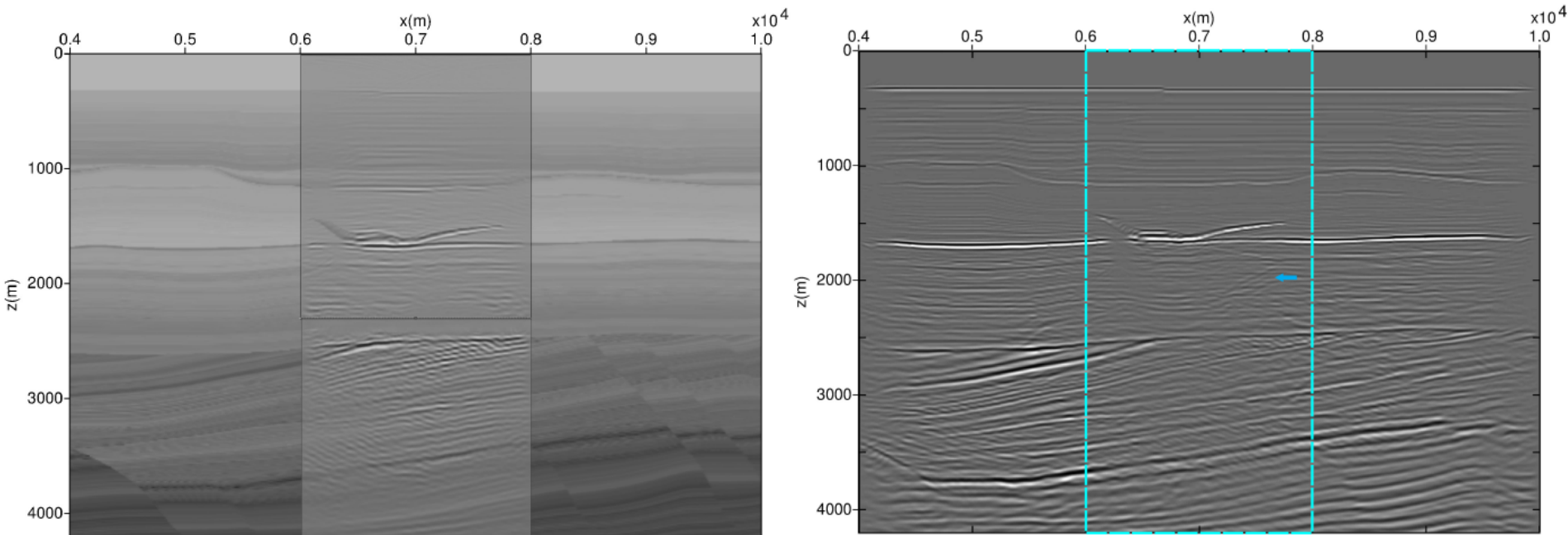


1



2

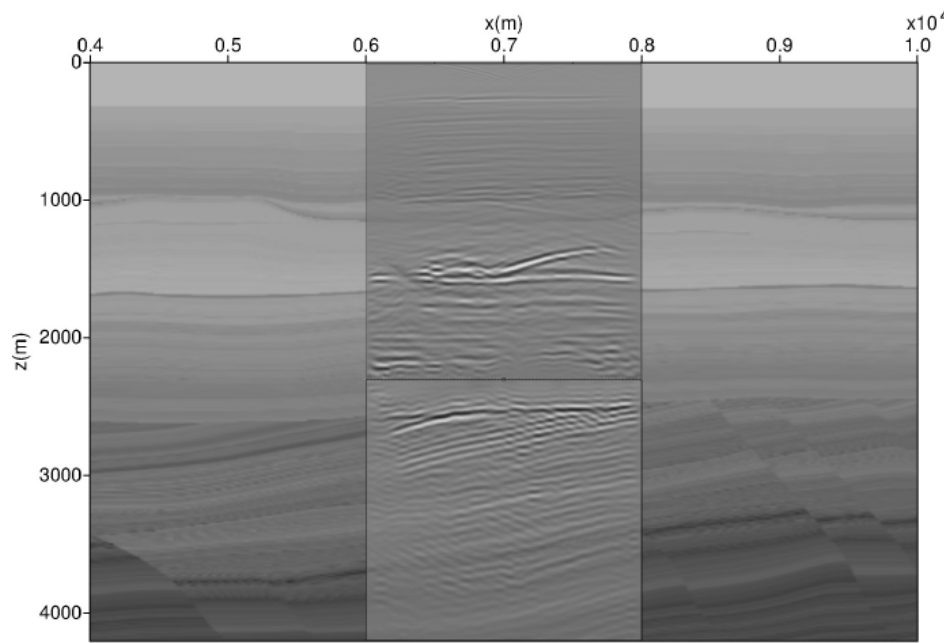
Example 2 – comparison (correct velocities)



Combined local image

Image from the surface

Example 2 – comparison (wrong velocities)



Combined local image

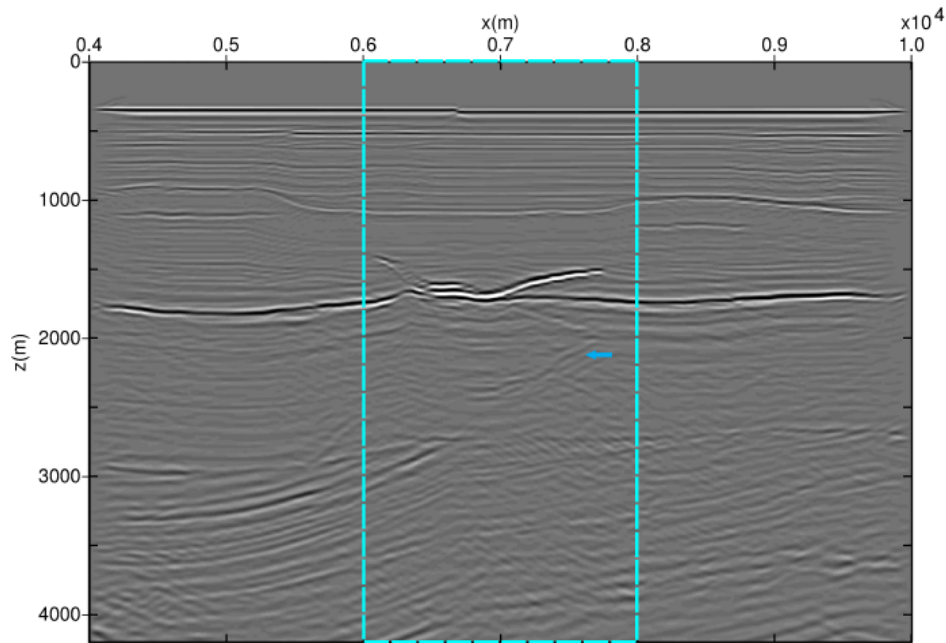


Image from the surface

Conclusions

- A new approach to **deep** imaging by combining surface and borehole seismic data;
- Only **single-component** data is needed;
- No macro-velocity model, completely **data-driven**;
- **Robust** images given wrong velocities;
- Better images without **internal multiples**.

Acknowledgements

- Research Council of Norway, ConocoPhillips, Det norske oljeselskap, Statoil, Talisman, TOTAL and Wintershall for financing through the research centre DrillWell
- ROSE consortium at NTNU
- Alexander Kritski for the synthetic velocity model

References

- Amundsen, L., 2001. Elimination of free-surface related multiples without need of the source wavelet, *Geophysics*, 66(1), 327–341.
- Broggini, F., Snieder, R., & Wapenaar, K., 2012. Focusing the wavefield inside an unknown 1D medium: Beyond seismic interferometry, *Geophysics*, 77(5), A25 – A28.
- Rose, J.H. [2002] “Single-sided” autofocusing of sound in layered materials. *Inverse Problems*, 1923–1934.
- Ravasi, M., Vasconcelos, I., Kritski, A., Curtis, A., da Costa Filho, C. A., & Meles, G. A., 2015. Marchenko imaging of volve field, north sea, 77th EAGE Conference and Exhibition, Extended Abstracts.
- Snieder, R., Miyazawa, M., Slob, E., Vasconcelos, I., & Wapenaar, K., 2009. A comparison of strategies for seismic interferometry, *Surveys in Geophysics*, 30(45), 503 – 523.
- Thorbecke, J. & Draganov, D., 2011. Finite-difference modeling experiments for seismic interferometry, *Geophysics*, 76(6), H1–H18.
- Thorbecke, J., Wapenaar, K., & Swinnen, G., 2004. Design of one-way wavefield extrapolation operators, using smooth functions in wlsq optimization, *GEOPHYSICS* , 69(4), 1037–1045.
- van der Neut, J. & Wapenaar, K., 2015. Point-spread functions for interferometric imaging, *Geophysical Prospecting*.
- van der Neut, J., Wapenaar, K., Thorbecke, J., & Slob, E., 2015b. Practical challenges in adaptive Marchenko imaging, 85th Annual Meeting, SEG, Expanded Abstracts.
- Wapenaar, K., Broggini, F., Slob, E., & Snieder, R., 2013. Three-dimensional single-sided Marchenko inverse scattering, data-driven focusing, Greens function retrieval, and their mutual relations, *Physical Review Letters*, 110(8), 084301.
- Wapenaar, K., Thorbecke, J., van der Neut, J., Broggini, F., Slob, E., & Snieder, R., 2014. Marchenko imaging, *Geophysics*, 79(3), WA39–WA57.